Spherical-Wave Computational AVO Modelling in Elastic and Anelastic Isotropic Two-Layer Media*

Arnim B. Haase[1] and Charles P. Ursenbach[1]

Search and Discovery Article #41564 (2015)
Posted February 23, 2015

*Adapted from extended abstract prepared in conjunction with a presentation given at CSPG/CSEG 2007 GeoConvention, Calgary, AB, Canada, May 14-17, 2007,

[1]University of Calgary, Calgary, AB, Canada (haaseab@ucalgary.ca)

Abstract

Compressional-wave AVO responses and converted-wave AVO responses in elastic and anelastic two-layer isotropic Class 1 models are investigated. These responses are computed by utilizing Zoeppritz reflection coefficients and the Weyl/Sommerfeld-integral. Spherical-wave depth dependence for PP and PSv Class 1 models is found to be strongest near the critical angle. The constant-Q approximation is used to introduce anelastic effects. AVO responses of two-layer isotropic models are sensitive to anelasticity. This Q-factor dependence is strongest near critical angles.

Introduction

Amplitude-versus-offset (AVO) analysis was introduced by Ostrander (1984). It is also discussed in a paper by Hron et al. (1986) as amplitude versus distance. AVO analysis and AVO inversion are now widely accepted tools in seismic exploration. Linear approximations of the Zoeppritz equations are commonly used to implement plane-wave analysis. Small incidence angles and small parameter changes are assumed for these approximations. At larger angles, linearized approximations begin to break down and they are not applicable near critical points. Even "exact Zoeppritz" is a plane-wave approximation to the real world. What, then, is the spherical-wave response for AVO Class 1? Krail and Brysk (1983) attempted to address this question, but incorporated a number of approximations, not all of which are valid at critical angles. The only approximation in the modelling study presented here is the assumption that compressional wave particle motion is parallel to the propagation direction and that converted-wave particle motion is perpendicular to the propagation direction.

Anelasticity of some degree is found in all rocks encountered in nature. Anelasticity causes attenuation and velocity dispersion of seismic waves. Velocity dispersion means velocities are functions of frequency. Frequency dependence of seismic velocities can be quantified by the frequency-independent quality factor Q (Kjartansson, 1979). This modelling study also seeks to quantify the sensitivity of Class 1 spherical-wave AVO responses with respect to finite Q-factors.

Potentials and Displacements

Plane-wave particle motion reflection and transmission coefficients for elastic isotropic media in welded contact are given by the Zoeppritz equations. The formalism for expressing spherical wave fronts as contour integrals over plane waves goes back to Weyl (1919). Aki and Richards (1980, p. 217) derive equations for generalized PP-reflections and generalized PSv-reflections in terms of potentials Φ (Equation 1) and Ψ (Equation 2):

$$\Phi = A i\omega e^{-i\omega t} \int_0^\infty R_{\mathrm{PP}}(p) \frac{p}{\xi} J_0(\omega p r) e^{i\omega\xi(z+h)} dp \tag{1}$$

$$\Psi = A i\omega e^{-i\omega t} \int_0^\infty \left(\frac{1}{i\omega p} \frac{\beta}{\alpha} R_{\mathrm{PS}}(p) \right) \frac{p}{\xi} J_0(\omega p r) e^{i\omega(\xi h + \eta z)} dp \tag{2}$$

[Notation is similar to Aki and Richards (1980).] Reflections from an elastic interface are computed firstly by introducing particle motion reflection coefficients given by the Zoeppritz equations. Secondly, particle motion *u* is computed from Equation (3)

$$u = \nabla\Phi + \nabla \times \nabla \times (0,0,\Psi) \tag{3}$$

and from the potentials given by Equations (1) and (2). Next, it is assumed that displacement is parallel to the ray direction for PP reflected waves, and perpendicular for converted waves. Other displacement components are neglected. [This is the sole approximation in the procedure and introduces very little error (Ursenbach et al., 2005).] The p-integrations proceed for a single frequency point. They are repeated for all frequency points desired in the output bandwidth, and then the time domain response is found by inverse Fourier transform. Quadrature traces are determined by Hilbert transform, and the maximum instantaneous amplitude yields the peak response at the receiver. When corrected for spherical spreading, this gives an estimate of the reflection coefficient.

Attenuation and Dispersion

A mathematical treatment of anelasticity can be found in Aki and Richards (1980). They show that causality requires velocity dispersion, for which they derive the following approximate expression:

$$v(\omega) = v_{ref} \left(1 + \ln\left(\omega / \omega_{ref} \right) \Big/ (\pi Q) - \frac{i}{2Q} \right) \tag{4}$$

where Q is a frequency-independent quality factor. The values v_{ref} and ω_{ref} are assumed known. As in the elastic case before, spherical-wave displacements *u* are computed from the potentials Φ and Ψ. The integrations shown in Equations 1 and 2 again proceed one frequency point at a time. However, in the anelastic situation velocities are complex and must be recomputed for every frequency point, according to Equation 4.

The P-wave quality factor for the top layer (Q_{P1}) is assumed to be known for the computations and is listed in the figures. Q_{P2} (for the bottom layer) as well as S-wave quality factors Q_{S1} and Q_{S2} are calculated with the aid of empirical equations (Waters, 1978; Udias, 1999):

$$1/Q_P = \left(\frac{const.}{\alpha}\right)^2, \tag{5}$$

$$Q_S = Q_P \frac{4}{3}\left(\frac{\beta}{\alpha}\right)^2 \tag{6}$$

Modelling Results

An actual gas-sand reservoir from the prairies is utilized to derive two-layer models for this study. Density ρ_1 is 2400 kg/m^3 for the layer just above the reservoir. P-wave velocity α_1 = 2000 m/s is dictated by a reservoir depth of 500 m and a corresponding two-way travel time of approximately 500 ms. The layer parameters for AVO Class 1 shown in Table 1 are adapted from Rutherford and Williams (1989). Output signal bandwidth and linear edge tapers are determined by choosing a 5/15-80/100 Hz Ormsby wavelet as the source signature. Free surface effects are not considered in this study. A P-wave point source and spherical incident wave fronts are assumed for the computations. The appearance of computed AVO results depends on scaling. Spherical spreading must be compensated for if results are to be compared to plane-wave responses. All normalization factors used to compute Figure 1 and Figure 3 are derived by setting reflection coefficients R in Equations 1 and 2 to unity. The *trace* displays (Figure 2 and Figure 4) are scaled individually in order to accommodate maximum amplitudes. Clipping of maximum trace amplitudes is indicated by colour changes. Figure 1 shows elastic AVO response magnitudes computed from trace envelopes. Figure 2 displays the corresponding spherical-wave traces, from which, after normalization, Figure 1 may be derived. The same two-layer model as was utilized in the elastic situation is also employed in the anelastic study. All velocities listed in Table 1 are taken to be reference velocities here; the reference frequency (see Equation 4) is set to 50 Hz. As before, a 5/15-80/100 Ormsby wavelet is chosen as the source signature; a P-wave point source is assumed. Free surface effects are ignored. Calculations are performed for two different values of the top layer P-wave quality-factor: firstly, Q_{P1} = 100 and, secondly, Q_{P1} = 387.5. The other Q-factors are calculated from Equations 5 and 6 and are listed in Table 2. Figure 3 and Figure 4 display the anelastic analogues to Figure 1 and Figure 2.

Discussion and Conclusions

For Class 1 AVO models, the P-wave velocity is increasing across the interface as can be seen in Table 1. Because of this velocity increase, a critical angle exists and head waves are generated in Class 1 models. A head wave can be seen separating from reflected waves at the highest angles in Figure 2b. Figure 1a shows the magnitude of R_{PP} for Class 1. The greatest departure from a plane-wave comparison is observed near the critical angle. Normalized Q-dependence for spherical-wave AVO Class 1, as shown in Figure 3, to some degree mimics normalized depth dependence of the elastic situation (see Figure 1). Increasing Q-factors and increasing depths move normalized spherical-wave AVO closer to plane-wave comparisons. In summary, exact spherical-wave reflection coefficients may be calculated numerically by integration over the planewave coefficients, R_{PP} and R_{PS}. Scaling by similar results obtained using unit reflectivity allows one to identify fundamental deviations

from plane-wave behaviour. Class 1 models show significant amplitude deviations near the critical angle. This is observed even at 2000m depth.

Acknowledgements

The authors thank Professor E. Krebes for helpful discussions related to the theory. Support from CREWES and its industrial sponsorship is gratefully acknowledged.

References Cited

Aki, K.T., and P.G. Richards, 1980, Quantitative Seismology: Theory and Methods: V. 1, W.H. Freeman and Co., 557 p.

Hron, F., B.T. May, J.D. Covey, and P.F. Daley, 1986, Synthetic seismic sections for acoustic, elastic, anisotropic, and vertically inhomogeneous layered media: Geophysics, v. 51/3, p. 710-735.

Kjartansson, E., 1979, Constant Q, wave propagation and attenuation: Journal of Geophysical Research, v. 84, p. 4737-4748.

Krail, P.M., and H. Brysk, 1983, Reflection of spherical seismic waves in elastic layered media: Geophysics, v. 48/6, p. 655-664.

Ostrander, W.J., 1984, Plane-wave reflection coefficients for gas sands at nonnormal angles of incidence: Geophysics, v. 49/10, p. 1637-1648.

Rutherford, S.R., and R.H. Williams, 1989, Amplitude-versus-offset variations in gas sands: Geophysics, v. 54/6, p. 680-688.

Udias, A., 1999, Principles of seismology: Cambridge University Press, p. 260.

Ursenbach, C.P., A.B. Haase, and J.E. Downton, 2005, An efficient method for AVO modeling of reflected spherical waves: 75th SEG meeting, Expanded Abstracts, p. 202-205.

Waters, K.H., 1978, Reflection Seismology: John Wiley and Sons, Inc., p. 203.

Weyl, H., 1919, Ausbreitung elektromagnetischer Wellen ueber einem ebenen Leiter: Ann. Physik, v. 60, p. 481-500.

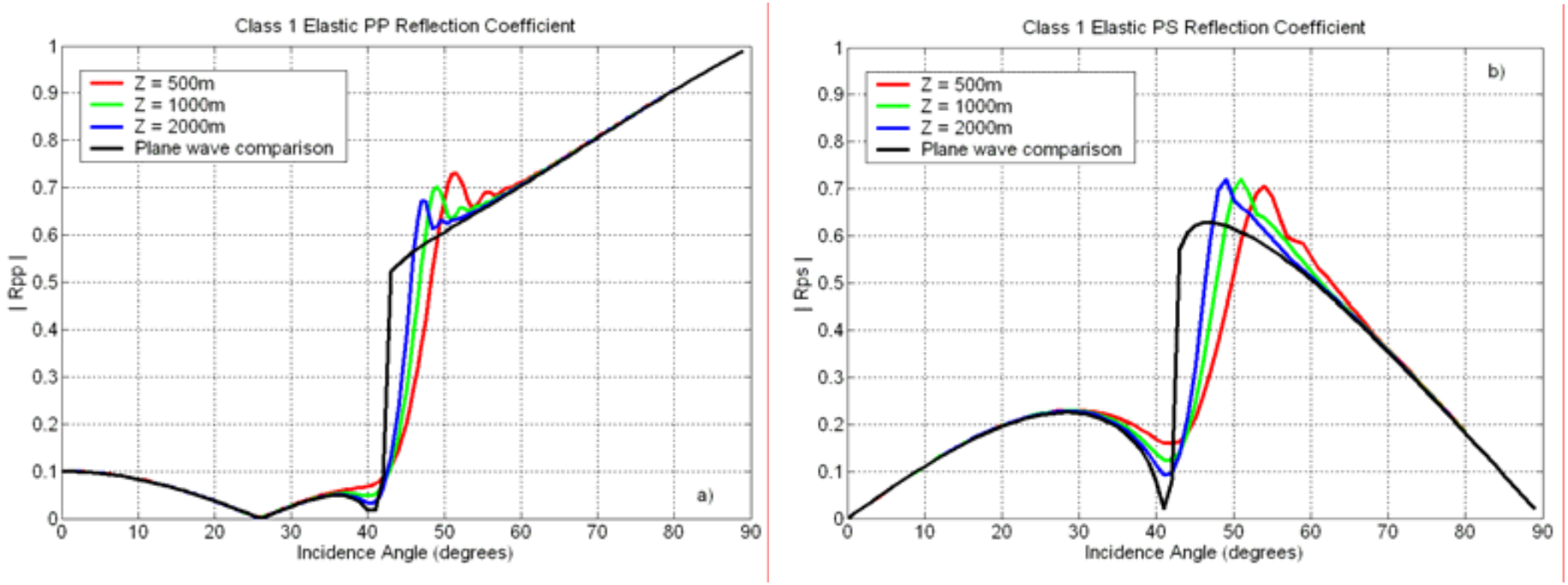

Figure 1. Spherical-wave reflection coefficients for Class 1 AVO, (a) PP (b) PSv.

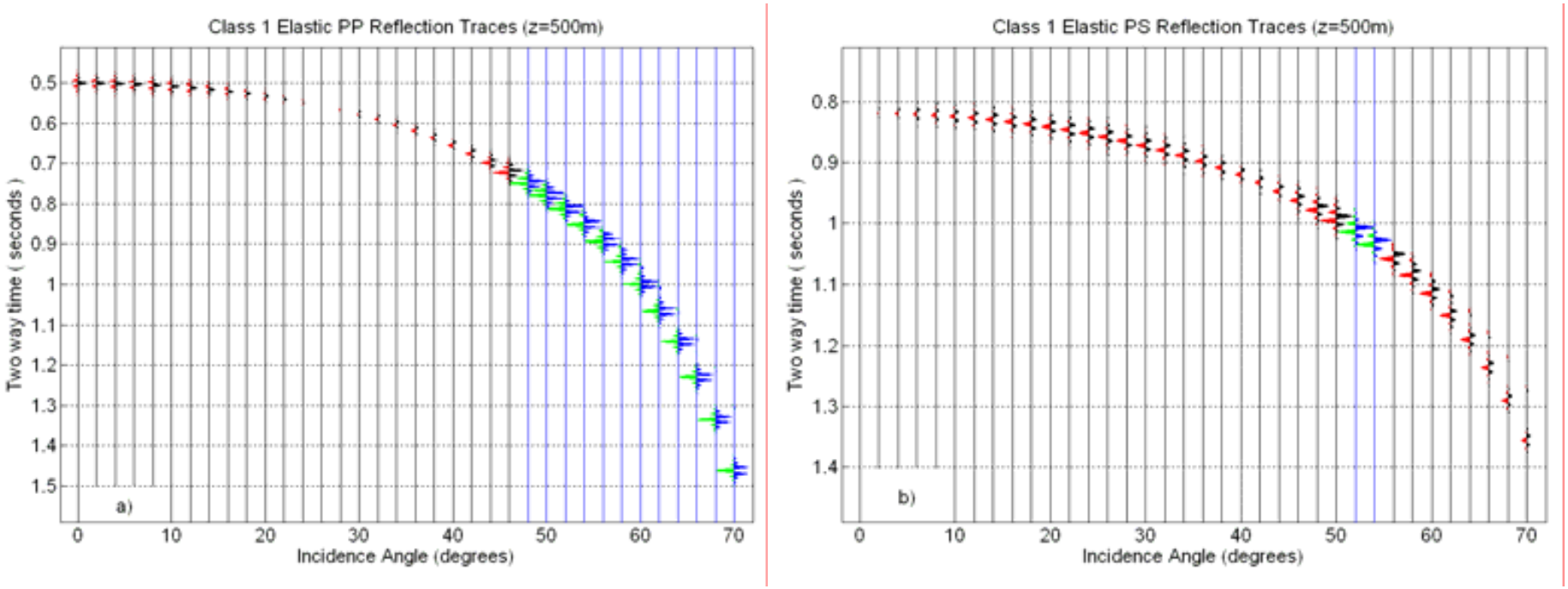

Figure 2. Spherical-wave reflection traces for Class 1 AVO, (a) PP (b) PSv.

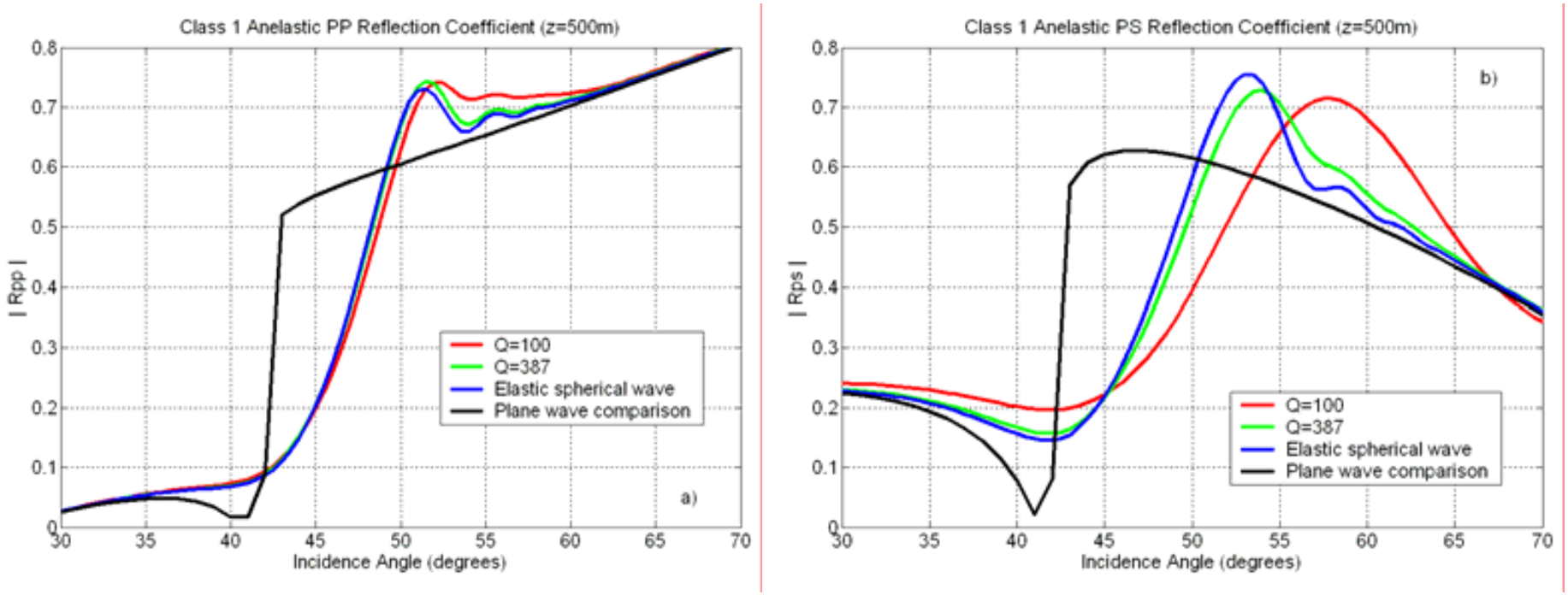

Figure 3. Anelastic spherical-wave reflection coefficients for Class 1 AVO, (a) PP (b) PSv.

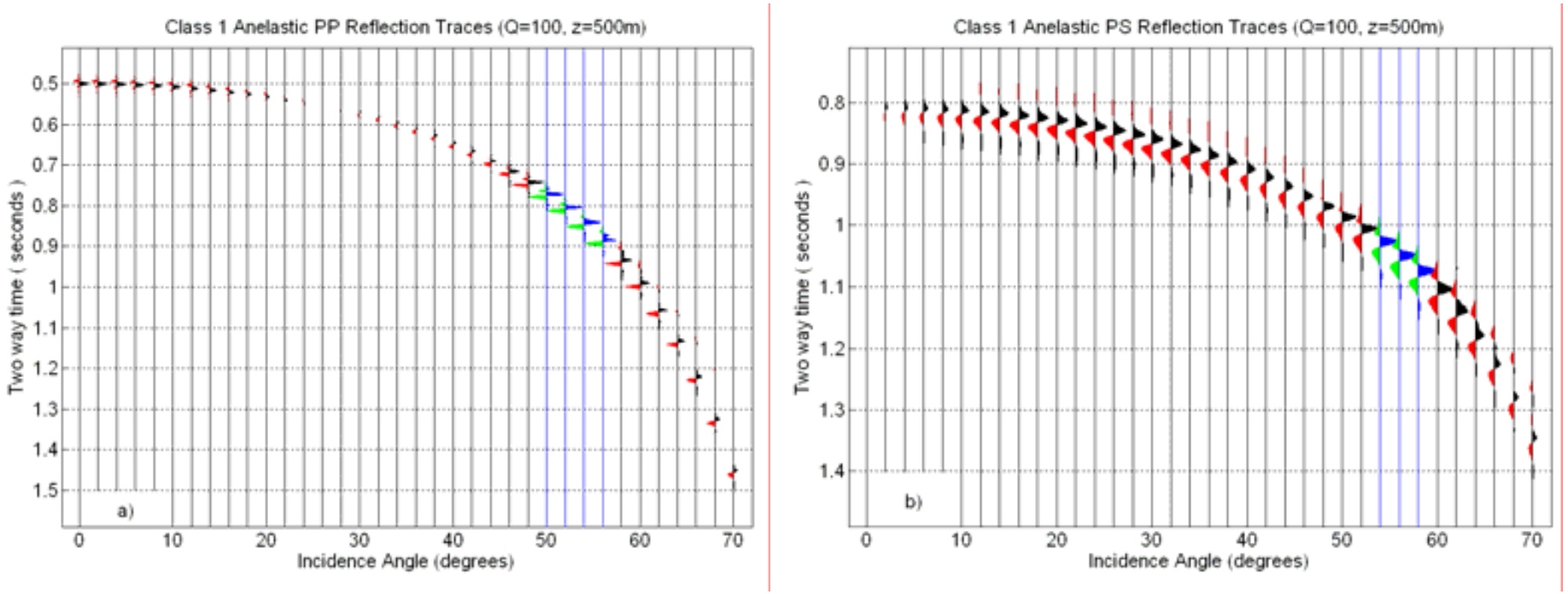

Figure 4. Anelastic spherical-wave reflection traces for Class 1 AVO, (a) PP (b) PSv.

α_1/[m/s]	β_1/[m/s]	ρ_1/[kg/m^3]	α_2/[m/s]	β_2/[m/s]	ρ_2/[kg/m^3]
2000	879.88	2400	2933.33	1882.29	2000

Table 1. Layer parameters.

Q_{p1}	Q_{p2}	Q_{s1}	Q_{s2}
100	215.1	25.8	118.1
387.5	833.5	100	457.6

Table 2. Derived Q-factors.